

PAPER • OPEN ACCESS

Testing fuel cell catalysts under more realistic reaction conditions: accelerated stress tests in a gas diffusion electrode setup

To cite this article: Shima Alinejad *et al* 2020 *J. Phys. Energy* **2** 024003

View the [article online](#) for updates and enhancements.



PAPER

OPEN ACCESS

RECEIVED

28 November 2019

REVISED

19 December 2019

ACCEPTED FOR PUBLICATION

6 January 2020

PUBLISHED

11 February 2020

Original content from this work may be used under the terms of the [Creative Commons Attribution 3.0 licence](#).

Any further distribution of this work must maintain attribution to the author(s) and the title of the work, journal citation and DOI.



Testing fuel cell catalysts under more realistic reaction conditions: accelerated stress tests in a gas diffusion electrode setup

Shima Alinejad¹, Masanori Inaba^{2,3}, Johanna Schröder¹, Jia Du¹, Jonathan Quinson², Alessandro Zana¹ and Matthias Arenz^{1,4}

¹ Department of Chemistry and Biochemistry, University of Bern, Freiestrasse 3, CH-3012 Bern, Switzerland

² Department of Chemistry, University of Copenhagen, Universitetsparken 5, DK-2100 Copenhagen Ø, Denmark

³ Toyota Central R&D Labs., Inc., Nagakute, Aichi 480-1192, Japan

⁴ Author to whom any correspondence should be addressed.

E-mail: matthias.arenz@dcb.unibe.ch

Keywords: accelerated stress tests, gas diffusion electrode, platinum, fuel cells, carbon supported high surface area catalysts

Supplementary material for this article is available [online](#)

Abstract

Gas diffusion electrode (GDE) setups have very recently received increasing attention as a fast and straightforward tool for testing the oxygen reduction reaction (ORR) activity of surface area proton exchange membrane fuel cell (PEMFC) catalysts under more realistic reaction conditions. In the work presented here, we demonstrate that our recently introduced GDE setup is suitable for benchmarking the stability of PEMFC catalysts as well. Based on the obtained results, it is argued that the GDE setup offers inherent advantages for accelerated degradation tests (ADT) over classical three-electrode setups using liquid electrolytes. Instead of the solid–liquid electrolyte interface in classical electrochemical cells, in the GDE setup a realistic three-phase boundary of (humidified) reactant gas, proton exchange polymer (e.g. Nafion) and the electrocatalyst is formed. Therefore, the GDE setup not only allows accurate potential control but also independent control over the reactant atmosphere, humidity and temperature. In addition, the identical location transmission electron microscopy (IL-TEM) technique can easily be adopted into the setup, enabling a combination of benchmarking with mechanistic studies.

1. Introduction

Benchmarking the activity and stability of proton exchange membrane fuel cell (PEMFC) catalysts using classical three-electrode setups and an aqueous electrolyte solution is a popular approach [1, 2]. The electrode potential can be controlled independently of the reaction conditions allowing not only comparison of the performance of different PEMFC catalysts, but also investigation into how potential excursions affect the catalyst stability and the degradation mechanism. For the latter, accelerated degradation tests (ADTs) are employed in combination with techniques such as identical location transmission and scanning electron microscopy (IL-TEM and IL-SEM) [3–12], and scanning flow cells (SFC) coupled to inductively coupled plasma—mass spectrometry (ICP-MS) [13, 14]. Thus, degradation mechanisms, such as metal dissolution and particle detachment, can be related to certain excursions in the electrode potential, as well as catalyst properties such as particle size and carbon support. The aim of ADTs therefore is to apply realistic conditions and at the same time reduce the time in which a performance loss is observed significantly [15–17]. Although this is a contradictory goal, certain ADT protocols are commonly accepted as a compromise, in particular one of the Fuel Cell Commercialization Conference of Japan's (FCCJ) [18, 19] simulating load-cycle and start-up/shutdown conditions of a PEMFC.

Despite the achievements made, the current approach also has disadvantages. For example, it is not clear if and how an aqueous electrolyte environment when compared to a realistic three-phase boundary of humidified reactant gas (proton exchange polymer, e.g. Nafion) influences the degradation of the active component and the carbon support, respectively. In the aqueous electrolyte environment it is found that for certain Pt/C fuel cell catalysts and simulated start-up/shutdown conditions the degradation mechanism is restricted to particle loss,

most likely due to carbon corrosion [3]. However, under simulated load-cycle conditions the main observed degradation mechanism changes to particle migration and coalescence [20]. By comparison, in membrane electrode assembly (MEA) tests the reported degradation mechanism is in general platinum dissolution [21], and in some cases extensive carbon corrosion. More subtle mechanisms, such as particle migration and coalescence, cannot be identified.

Only few efforts exist that combine a simple setup with a more realistic environment [22–29]. Here, we demonstrate how our recently introduced gas diffusion electrode (GDE) setup [30–32] can be used for benchmarking the stability of high surface PEMFC catalysts under realistic reaction conditions. Gas diffusion electrode setups have very recently received increasing attention allowing one to combine the ease of use known from electrochemical three-electrode setups and liquid aqueous environments with reaction conditions closer to applications [33]. In the work presented, it is shown that in the GDE setup parameters such as the reactant gas atmosphere and its humidity can be easily controlled, and their influence on the catalyst stability can be studied. Thus, the setup offers inherent advantages over the conventional three-electrode setups for ADTs. In addition, the IL-TEM technique can easily be adopted into the setup, enabling a combination of stability benchmarking with mechanistic studies.

2. Experimental

2.1. Chemicals, materials and gases.

Ultrapure water (resistivity $>18.2 \text{ M}\Omega \cdot \text{cm}$, total organic carbon (TOC) $<5 \text{ ppb}$) from a Milli-Q system (Millipore) was used for acid/base dilutions, catalyst ink formulation and the GDE cell cleaning. The following chemicals were used in ink formulation and electrolyte preparation: isopropanol (IPA, 99.7 + %, Alfa Aesar), 70% perchloric acid (HClO_4 , Suprapur, Merck), potassium hydroxide hydrate ($\text{KOH} \cdot \text{H}_2\text{O}$, Suprapur, Merck), commercial Pt/C catalysts (46.0 wt% TEC10E50E and 50.6 wt% TEC10E50E-HT, Tanaka kikinzo kogyo, as well as HISPEC 3000, Johnson Matthey) and Nafion dispersion (D1021, 10 wt%, EW 1100, Fuel Cell Store). A Nafion membrane (Nafion 117, 183 μm thick, Fuel Cell Store) and a gas diffusion layer (GDL) with a microporous layer (MPL) (Sigracet 39BC, 325 μm thick, Fuel Cell Store) were employed in the GDE cell measurements. Before use, the Nafion membrane was prepared and activated as follows: after cutting several circles with a diameter of 2 cm from a sheet of Nafion membrane, the membranes were treated for 30 min at 80 °C in 5 wt% H_2O_2 , followed by rinsing with Milli-Q water. Then, the membranes were treated for 30 min at 80 °C in Milli-Q water followed by rinsing with Milli-Q water. Finally, the membrane was treated for 30 min at 80 °C in 8 wt% H_2SO_4 , again followed by rinsing with Milli-Q water. All membranes were kept in a glass vial filled with Milli-Q water. The following gases from Air Liquide were used in electrochemical measurements: Ar (99.999%), O_2 (99.999%) and CO (99.97%). TEM characterization of the respective Pt/C catalysts can be found in the supporting information (figure S1 is available online at stacks.iop.org/JPENRGY/2/024003/mmedia).

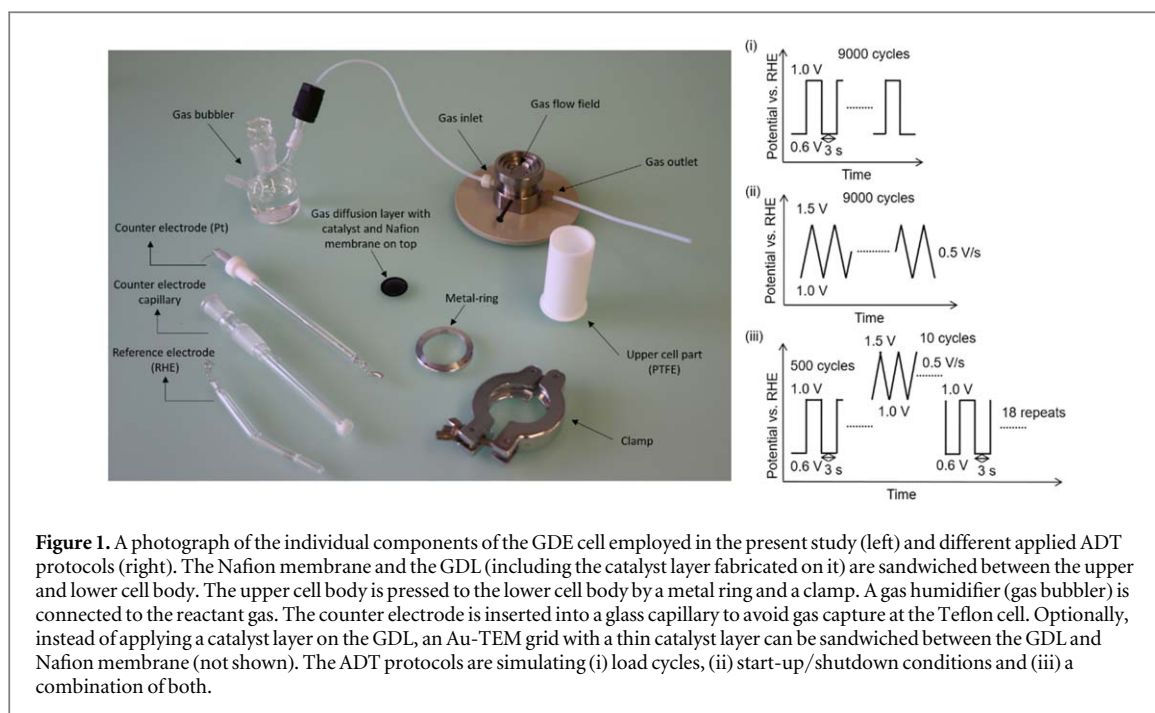
2.2. Gas diffusion electrode cell setup.

An in-house developed GDE cell setup was employed in all electrochemical measurements that was initially designed for measurements in hot phosphoric acid [24]. The design used in the present study has been described before [31]. In short, it was optimized to low temperature PEMFC conditions ($<100 \text{ }^\circ\text{C}$) by placing a Nafion membrane between the catalyst layer and liquid electrolyte; no liquid electrolyte is in direct contact with the catalyst [31]. A photograph of the parts of the improved GDE setup is shown in figure 1.

The cell body above the Nafion membrane is made of polytetrafluoroethylene (PTFE). A platinum mesh and a reversible hydrogen electrode (RHE) were used as a counter electrode and a reference electrode, respectively. The counter electrode was placed inside a glass capillary tube with a glass frit on the bottom, which avoids the trapping of gas bubbles in the hole of the Teflon cell and consequently helps to increase the reproducibility of the measurement. All potentials in this study are referred to the RHE potential. For initial cleaning, the Teflon upper part was soaked in mixed acid ($\text{H}_2\text{SO}_4\text{:HNO}_3 = 1:1$, v-v) overnight. Subsequently, it was rinsed thoroughly with ultrapure water, and boiled in ultrapure water twice. Between the measurements, the Teflon upper part was boiled in ultrapure water twice.

2.3. Catalyst ink formulation and catalyst layer application.

Here, 2.0 mg of the respective commercial 46.5 wt% Pt C^{-1} catalyst powder and 10.09 μl (or 936 μl) of the 10 wt% Nafion dispersion were mixed with 4.74 ml (or 5.15 ml) of IPA:ultrapure water (1:3, v-v) mixed solvent. The glass vial containing the mixture was placed in the ultrasonic bath and sonicated for 15 min. Subsequently, the mixture was dispersed using a horn sonicator (Q500, QSonica) for 1 min. Before the application of the catalyst ink on the GDL, circular pieces (dia. = 20 mm) of the GDL were punched from a larger sheet. The catalyst ink was sprayed onto the GDL (MPL-coated side) using a pump (Harvard apparatus 11 plus) with a



flow rate of 0.5 ml min^{-1} and an ultrasonic spray nozzle (Sonozap narrow spray atomizer). During the spraying, the catalyst ink was constantly sonicated by an ultra sonicator (Sonozap ultrasonic atomizer) with a power of 1.5 W and frequency of 130 KHz, and the GDL was heated on a heating plate (140°C) and covered with an iron mask so that a circular catalyst layer (dia. = 3 mm) was formed at the center of the GDL.

2.4. Electrochemical measurements.

The electrochemical measurements were performed using a computer controlled potentiostat (ECi 200, Nordic Electrochemistry). The measurements were performed with 4 M HClO_4 aqueous solution in the upper Teflon compartment of the GDE setup by applying different temperatures, as reported previously [31]. Prior to the measurements, the electrode was purged from the backside (through the GDL) with Ar gas, and the catalyst was cleaned by potential cycles between 0.06 and $1.10 \text{ V}_{\text{RHE}}$ at a scan rate of 500 mV s^{-1} until a stable cyclic voltammogram (CV) could be observed (~ 50 cycles). The resistance between the working and reference electrode ($\sim 10 \Omega$) was compensated to an effective value of around 1Ω using the analog positive feedback scheme of the potentiostat. The resistance was determined online using an AC signal (5 kHz, 5 mV) [34].

To determine the stability of the Pt/C electrocatalysts, ADTs inspired by the FCCJ [18] were performed. Three different ADT protocols were tested: (i) a protocol simulating load cycles, where the electrode potential was modulated with a square wave and stepped between 0.6 and $1.0 \text{ V}_{\text{RHE}}$ with a holding time of 3 s at each voltage for a total of 9000 potential cycles; (ii) a protocol simulating start-up/shutdown conditions [35], where the electrode potential was cycled with a scan rate of 0.5 V s^{-1} between 1.0 and $1.5 \text{ V}_{\text{RHE}}$ for a total of 9000 potential cycles; and (iii) a mixed protocol combining (i) and (ii), which consisted of 500 potential cycles of the load-cycling protocol followed by 10 potential cycles of the start-up/shutdown protocol, repeated overall 18 times (in the following we refer to this protocol as the mixed protocol). To monitor the H_{upd} area and the change in the quinone/hydroquinone (Q/HQ) redox peak [36, 37] after each 1000 potential cycles (500 cycles for procedure (iii)) six CVs were recorded in an Ar atmosphere at a scan rate of 0.5 V s^{-1} . The electrochemically active surface area (ECSA) of the catalyst was determined by conducting CO stripping voltammetry before and after the ADT. We did not record further CO stripping during the ADT to minimize the potential negative impact of CO stripping on the surface area [38–40]. For the CO stripping measurements, the working electrode was held at 0.05 V while purging first CO through the GDL for 5 min and thereafter Ar for an additional 5 min. The ECSA was determined from the CO (Q_{CO}) oxidation charge recorded at a scan rate of 50 mV s^{-1} . Unless otherwise stated, all measurements were performed at room temperature.

2.5. TEM grid preparation.

For IL-TEM investigations, a gold finder grid (400 mesh; Plano, Germany) was used. The catalyst ink was diluted by a factor of 1:10. Next, $10 \mu\text{l}$ of diluted catalyst ink was pipetted onto the gold finder grid. To avoid overlapping of the catalyst particles, after approximately 10 s the droplet of the catalyst was carefully absorbed off the grid with a filter paper. Then, the grid was dried, and the catalyst investigated in a Technai Spirit (FEI) with an

accelerating voltage of 80 kV before and after the ADT. The TEM grid was placed between a Nafion membrane and a GDL (without a catalyst layer on it) during the ADT. The ADT for the IL-TEM experiment was conducted by applying the load-cycling protocol (1200 cycles) at 60 °C, 100% relative humidity (RH).

3. Results and discussion

3.1. Comparison of different ADT protocols.

The aim of the present study was to employ our recently developed GDE setup mimicking the PEMFC environment to ADT studies. At first, we compared different ADT protocols for their suitability for monitoring the catalyst degradation in the GDE setup. The different ADT protocols are designed to apply as realistic conditions as possible, and at the same time to significantly reduce the time in which a performance loss is observed. For PEMFCs, a variety of different ADT protocols can be found in the literature. Here, we tested the popular approach suggested by the FCCJ [18, 19] simulating load-cycle and start-up/shutdown conditions, respectively. Load-cycle conditions are simulated by stepping the applied electrode potential between 0.6 and 1.0 V_{RHE} and holding the potential for three seconds each. The 0.6 V_{RHE} is a typical cell potential under full load, whereas 1.0 V_{RHE} is close to the open circuit potential of Pt and represents the cell voltage under idle conditions. Start-up/shutdown conditions are simulated by scanning the applied electrode potential between 1.0 and 1.5 V_{RHE} with a scan rate of 0.5 $V s^{-1}$, which simulates an increase in cathode potential when introducing hydrogen in an air-filled flow field or replacing the hydrogen with air during the start-up and shutdown period, respectively [35]. For a better understanding of the ADT protocols the reader is referred to [18]. The total duration of the load-cycle treatment lasted 9000 cycles, which is a total of 16 and 19 h in Ar and O_2 atmosphere, respectively. The degradation is monitored by CVs recorded in an Ar atmosphere after each 1000 cycles, as well as CO stripping experiments before and after the ADT protocol (therefore, the total time varies as for the ADT protocol measured in Ar and O_2 , respectively, as the O_2 needed to be replaced from the flow field before measuring the CVs). The start-up/shutdown treatment lasted 9000 cycles as well, which is a total of 6 and 9 h in Ar and O_2 atmospheres, respectively.

In figure 2 the effect of both ADT protocols employed in the GDE setup is demonstrated on a commercial Pt/C catalyst with an average particle size of 2–3 nm; see figure S1. On the left-hand side, the CVs recorded every 1000 cycles in an Ar atmosphere are plotted, whereas on the right-hand side, the CO stripping curves recorded before and after the ADT treatment are shown. For Pt/C, the ECSA loss can be monitored based on the changes in the H_{upd} area in the CVs recorded in an Ar atmosphere, as well as changes in the area under the CO stripping curves. Further information concerning the degradation of the catalyst can be derived from the change in the 'oxide region' ($\sim 0.75 V_{RHE}$) and the formation of a Q/HQ redox peak ($\sim 0.6 V_{RHE}$). As seen in figures 2(a), (b), the behavior of the Pt/C catalyst upon the load-cycling treatment (i) is qualitatively the same as reported previously for ADT measurements performed in half-cells with a liquid electrolyte [37]. The Pt/C catalyst continuously loses ECSA, and the reduction peak in the 'oxide region' decreases, whereas its peak potential slightly shifts to higher potentials. After 9000 cycles a total loss in ECSA of $41.5 \pm 2.3\%$ is determined. Interestingly, this is roughly 10% more loss than what is observed for the same catalyst in a conventional cell with a liquid electrolyte ($32.0 \pm 1.6\%$); see table 1 and figures S2, 3 for a summary of the ECSA losses observed for different catalysts and under different conditions.

In contrast to protocol (i), the effect of applying the start-up/shutdown protocol (ii) in the GDE setup is more difficult to compare with previous measurements using conventional half-cells and liquid electrolytes [20, 37, 41]. When applying protocol (ii) in the GDE setup, see figures 2(c), (d), the CVs recorded in the Ar atmosphere quickly lose the features of Pt/C and become significantly tilted with time. This indicates massive carbon corrosion and an increase in cell resistance with time, which is confirmed by the online superposition of an AC signal (5 kHz, 5 mV). The same trend is seen in the CO stripping curve recorded after the ADT procedure. Due to the significant distortion of the CVs and CO stripping measurements a proper analysis of the surface area loss from determination of the H_{upd} or the CO stripping charge is highly questionable. Most likely the prolonged exposition to high electrode potentials leads to the massive oxidation not only of the catalyst layer, but also the MPL, and possibly even the GDL. Note that in our measurements the amount of carbon in the catalyst layer is significantly less than the carbon in the MPL.

A more representative degradation of the catalyst is achieved by the presented mixed ADT protocol (iii), which combines load cycles with start-up/shutdown cycles in a sequence of load cycles and start-up/shutdown events, figures 2(e), (f). Although only a limited number of high potential excursions are applied, the evolving features in the CV recorded every 1000 cycles are distinctively different to those in the load-cycle protocol (i): i.e. the CVs exhibit a strong increase in double layer capacitance, and the formation of a pronounced Q/HQ redox peak is observed. Although, also for this ADT, it cannot be excluded that the observed features are related to the degradation of the catalyst layer as well as the MPL and the GDL, the loss in the CO stripping area is solely related

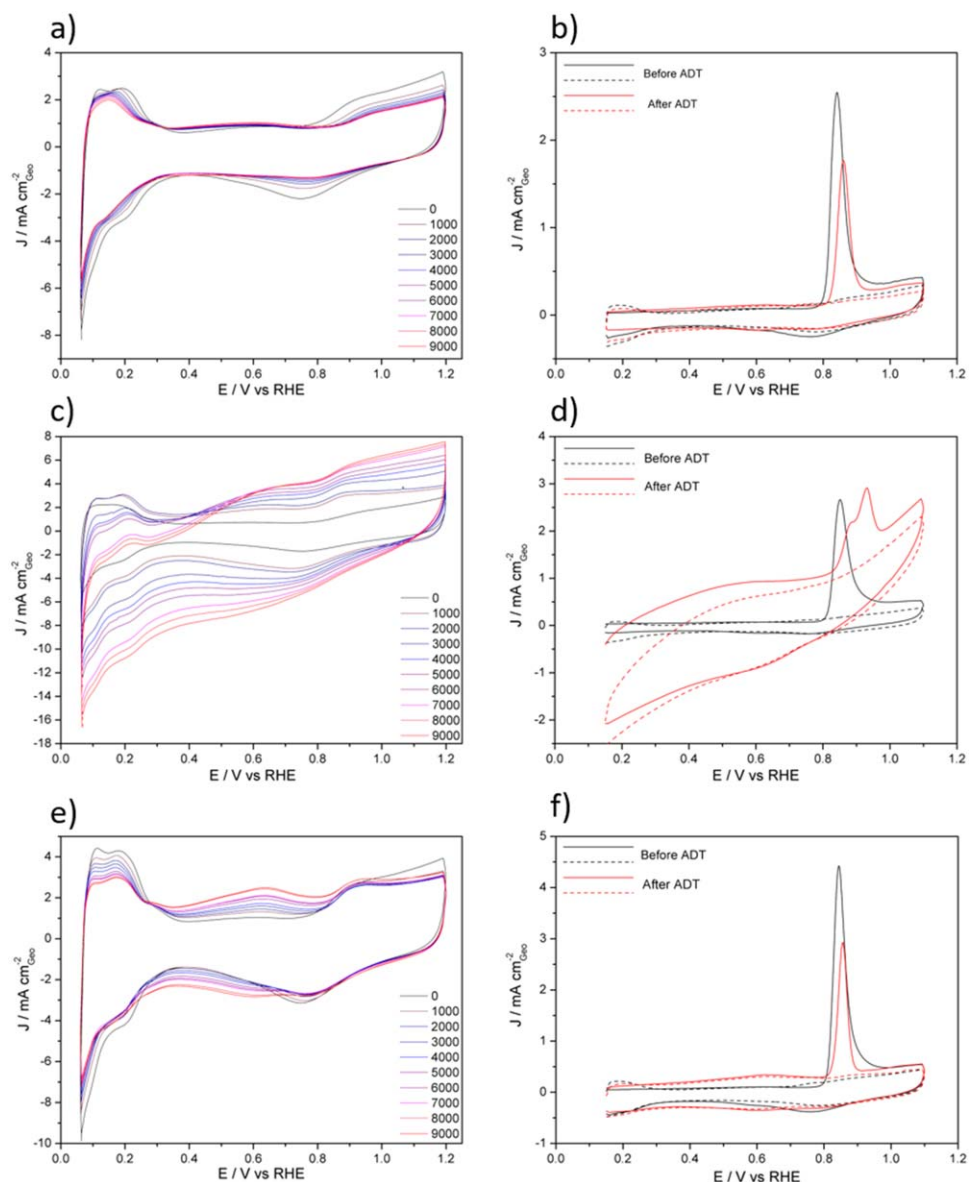


Figure 2. The influence of different ADT protocols performed in an Ar atmosphere on the electrochemical behavior of a commercial Pt/C catalyst (TEC10E50E). On the left-hand side, the CVs (sweep rate 0.5 V s^{-1}) recorded every 1000 cycles in Ar atmosphere are shown, whereas on the right-hand side, the initial and final CO stripping curves are shown (solid line) together with the subsequent CV (dashed line); both were recorded at a sweep rate of 0.05 V s^{-1} . (a), (b) The step protocol simulating load cycles; (c), (d) the CV protocol simulating start-up/shutdown conditions; (e), (f) the mixed protocol combining the two prior protocols. The measurements were performed at room temperature.

Table 1. The total percentage loss in ECSA during the different ADT protocols as determined from the CO stripping measurements. The error is the standard deviation of three independent measurements.

Catalyst	Cell type	ADT protocol	ECSA loss/%	
			Gas Atmosphere	
			Ar	O ₂
TEC10E50E	Conventional cell	load-cycle protocol (i)	32.0 ± 1.6	37.2 ± 2.5
TEC10E50E	GDE cell	load-cycle protocol (i)	41.5 ± 2.3	48.1 ± 1.6
		mixed protocol (iii)	54.3 ± 0.1	57.4 ± 1.8
TEC10E50E-HT	GDE cell	load-cycle protocol (i)	19.2 ± 0.5	18.2 ± 1.2
		mixed protocol (iii)	20.7 ± 0.4	24.0 ± 1.5

to the loss in the ECSA of the catalyst. In contrast to the commonly applied start-up/shutdown protocol (ii), the measurements from the mixed ADT protocol can be analyzed with confidence, and thus we suggest using such a mixed procedure instead of the protocol (ii) proposed by the FCCJ for simulating start-up/shutdown conditions. Despite the fact that the catalyst experiences only 180 high potential excursions in total, it is seen that in the mixed protocol (iii) the ECSA loss ($54.3 \pm 0.1\%$) is more than 10% higher than upon applying the load-cycle protocol (i) ($41.5 \pm 2.3\%$); see table 1.

3.2. The influence of the particle size and heat treatment.

We performed the same measurements (ADT protocol (i) and protocol (iii)) on an additional commercial catalyst (TEC10E50E-HT) with larger particle size, i.e. $\sim 4\text{--}5$ nm instead of $2\text{--}3$ nm, see figure S1. As expected and shown previously in ADT using conventional electrochemical cells [42], the results obtained in the GDE setup demonstrate a significantly higher loss in ECSA for the catalyst with a smaller particle size ($2\text{--}3$ nm, TEC10E50E) than for the one with a larger particle size ($4\text{--}5$ nm, TEC10E50E-HT). Upon applying the load-cycling protocol (i) using the Pt/C catalyst with $4\text{--}5$ nm particle size, the ECSA loss is $19.2 \pm 0.5\%$, i.e. it is reduced to less than half compared to the Pt/C with $2\text{--}3$ nm particle size (ECSA loss of $41.5 \pm 2.3\%$). When applying the mixed protocol (iii) the stability improvement is even more significant, i.e. an ECSA loss of $20.7 \pm 0.4\%$ is detected compared to $54.3 \pm 0.1\%$. An obvious explanation for the observed stability improvement is the larger particle size of the active Pt phase. It should be mentioned, however, that the particle size might not be the only contributing factor to the enhanced stability. As these are commercial samples, the exact synthesis routes are not publicly available; the catalyst notation, however, suggests that the larger particle size results from a heat treatment of the Pt/C catalyst with $2\text{--}3$ nm particle size. Such treatments result not only in increased particle sizes due to agglomeration and sintering, but also influence the carbon support properties [43]. For a more detailed study of the influence of the particle size on the catalyst stability, which is not within the scope of this work, therefore, the use of in-house synthesized catalysts using the toolbox approach [44] is suggested.

3.3. The influence of the reactant gas conditions.

The above-discussed ADT measurements were performed under an Ar atmosphere. Performing the same measurements in an O₂ atmosphere using the Pt/C catalyst with $2\text{--}3$ nm particle size leads to small but distinctive differences; see figure 3. The start-up/shutdown protocol (ii) faces the same limitations as when performed in the Ar atmosphere, and is therefore not discussed further. However, in the CVs of the load-cycle protocol (i), it can be seen that (compared to the ADT protocol (i) performed in the Ar atmosphere) the formation of the Q/HQ redox peak is more pronounced, indicating an impact of the O₂ atmosphere on the carbon support oxidation. This is confirmed in the CO stripping measurements, where a small but distinctive difference in ECSA loss is seen whether the ADT protocol is performed in an Ar ($41.5 \pm 2.3\%$) or O₂ ($48.1 \pm 1.6\%$) atmosphere. Interestingly, the difference in ECSA loss between measurements performed in Ar and O₂ atmospheres is less pronounced when applying the mixed ADT protocol (iii). This finding might be related to the fact that during the high potential excursions the catalyst experiences enhanced oxidation, independently of the reacting atmosphere. However, applying the same procedures (i) and (iii) with the Pt/C catalyst with $\sim 4\text{--}5$ nm particle size (TEC10E50E-HT), no influence of the reaction gas atmosphere on the recorded ECSA loss is discernible, i.e. $19.2 \pm 0.5\%$ in Ar and $18.2 \pm 1.2\%$ in O₂ gas atmosphere. The results therefore confirm previous reports stating that the gas atmosphere affects the surface chemistry of the carbon supports [28, 45], but they also show that the influence of the gas atmosphere on the ECSA losses is individually dependent on the Pt/C catalyst.

3.4. Influence of reactant gas humidity.

Another interesting factor in the degradation of PEMFC catalysts is the effect of the relative gas humidity. This factor is not accessible in standard electrochemical three-electrode setups with liquid aqueous electrolytes but can be easily studied in the GDE setup. To demonstrate the effect of the relative gas humidity, we performed a load-cycle ADT in dry oxygen gas (protocol (i)). To be able to monitor the real loss in ECSA, before and after the ADT, CO stripping measurements were performed in humidified gas. The results are summarized in figure 4. It is seen that in dry Argon gas, the H_{upd} region in the CVs—recorded as part of the load-cycle protocol (i)—decreases, indicating a significant reduction in active Pt surface area. This sudden loss in active Pt surface area can be correlated to a significant deactivation in dry gas conditions. However, the final CV recorded under re-humidified conditions demonstrates that the active Pt surface area can, to a large extent, be recovered. That is, after applying the load-cycle protocol (i) on the TEC10E50E Pt/C catalyst with a particle size of $2\text{--}3$ nm, the ECSA loss in dry O₂

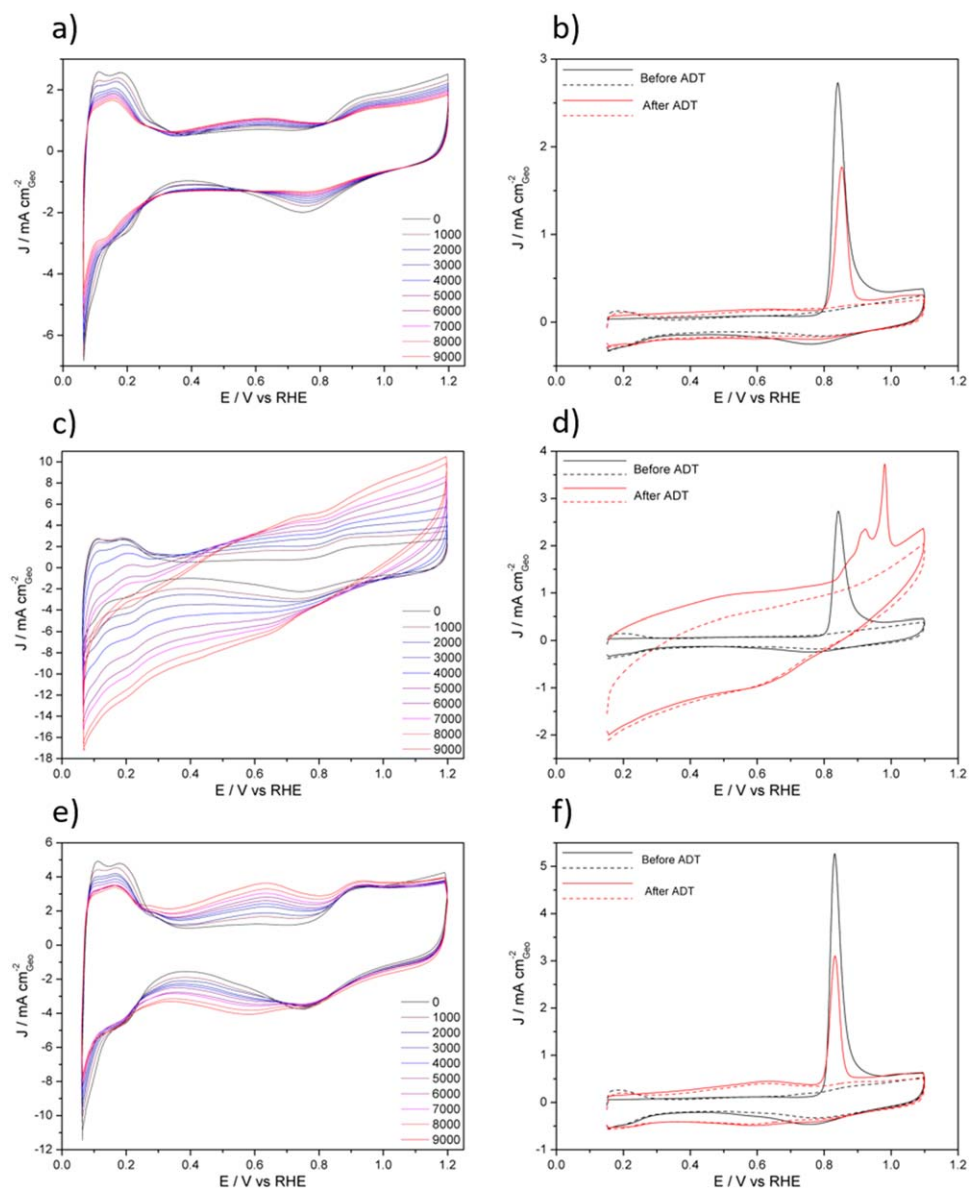


Figure 3. The influence of different ADT protocols performed in an O_2 atmosphere on the electrochemical behavior of a commercial Pt/C catalyst (TEC10E50E). On the left-hand side, the CVs (sweep rate 0.5 V s^{-1}) recorded every 1000 cycles in an Ar atmosphere are shown, whereas on the right-hand side, the initial and final CO stripping curves (solid line) are shown together with the subsequent CV (dashed line); both were recorded at a sweep rate of 0.05 V s^{-1} . (a), (b) The step protocol simulating load cycles; (c), (d) the CV protocol simulating start-up/shutdown conditions; (e), (f) the mixed protocol combining the two prior protocols. The measurements were performed at room temperature.

gas conditions was $\sim 50\%$, whereas switching back to humidified O_2 gas, the overall ECSA loss is only $\sim 28\%$, which is less than when applying the load-cycle protocol (i) under fully humidified conditions.

The results can be interpreted in the following way. During the load-cycle protocol (i), the active Pt surface area is significantly reduced due to a loss in proton conduction from the dry Nafion in the catalyst layer. Thus, only part of the catalyst is actually subjected to degradation while the other part remains unaltered. This results in an overall lower degradation when switching back to fully humidified conditions. Such behavior, however, is not expected in real PEMFC devices, where the power output is decisive. In contrast to the potentiostatic ADT measurements, under amperometric conditions, inaccessible Pt surface area due to dry gas conditions is expected to lead to increased degradation in the accessible part of the catalyst layer. To demonstrate this, we designed an amperometric ADT protocol that switches 600 times from load (i.e. $100 \text{ mA cm}^{-2}_{\text{geo}}$) to open circuit potential (OCP) and back, holding the respective conditions for 3 s each. Comparing the same TEC10E50E Pt/C catalyst under dry and humidified conditions, respectively, a significantly higher ECSA loss was observed for the dry O_2 gas ($\sim 65\%$ loss) compared to the humidified O_2 gas ($\sim 10\%$ loss) conditions. In contrast to the potentiodynamic load-cycle protocol (i), re-humidifying the catalyst after applying the

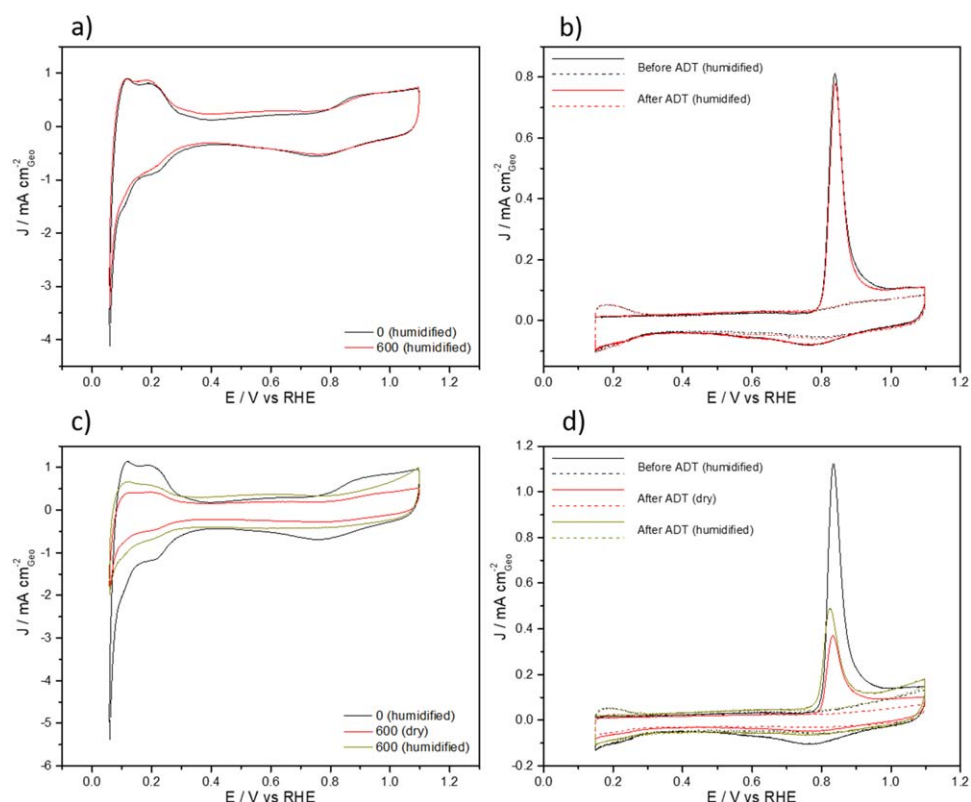


Figure 4. The influence of humidification of O_2 gas on the ECSA loss of a commercial Pt/C catalyst (TEC10E50E) upon applying an amperometric ADT consisting of 600 steps between load conditions ($100 \text{ mA cm}^{-2}_{\text{geo}}$) and OCP, maintaining each condition for 3 s each. (a), (b) CVs and CO stripping (sweep rate 0.05 V s^{-1}) before and after the ADT protocol applied under humidified O_2 gas. (c), (d) CVs and CO stripping (sweep rate 0.05 V s^{-1}) before and after the ADT protocol applied under dry O_2 gas. The measurements before applying the ADT protocol were recorded under humidified conditions. In addition, the effect of re-humidifying the O_2 gas after applying the ADT protocol is shown. The measurements were performed at room temperature.

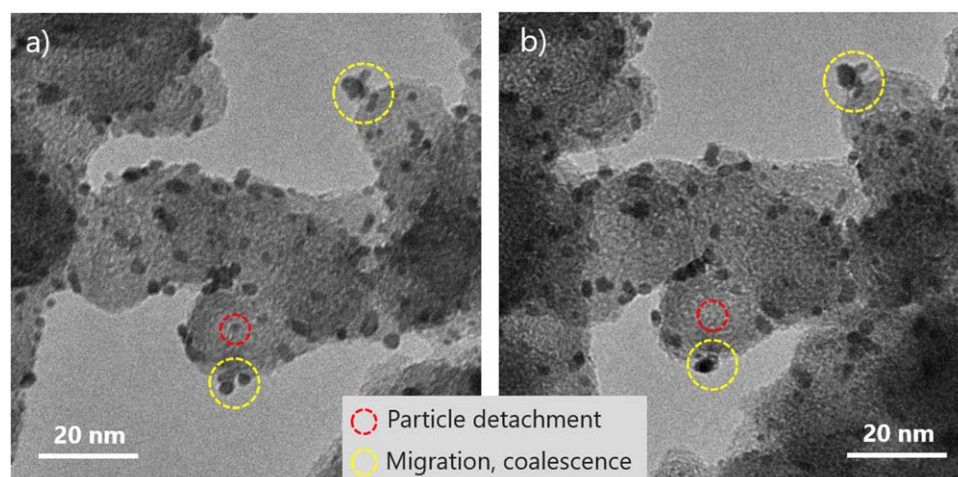


Figure 5. IL-TEM micrographs of a commercial 20 wt% Pt C^{-1} catalyst (HiSPEC 3000) (a) before and (b) after load-cycle ADT treatment for 1200 cycles at 60°C .

amperometric ADT protocol could only recover a small part of the ECSA (total loss of $\sim 57\%$ instead of $\sim 65\%$ loss).

3.5. IL-TEM measurements in the GDE setup.

An advantage of half-cells with a liquid electrolyte—compared to MEA test—is the possibility of performing IL-TEM measurements to analyze the degradation mechanism leading to the loss in active surface area. Here, we demonstrate that the same is feasible in the GDE setup, and even elevated temperatures can be used; see figure 5.

By placing the TEM grid between the membrane electrolyte and GDL, the IL-TEM method can be applied straightforwardly. For the demonstration, a catalyst with lower Pt loading (20 wt%) was used to facilitate the ability to follow the change in individual particles. The typical degradation phenomena, such as migration and coalescence (yellow circles) and particle detachment (red circle), can be clearly seen to occur as consequence of the load-cycle treatment.

4. Conclusion

We demonstrate the application of our recently introduced GDE setup for benchmarking the stability of PEMFC catalysts under realistic reaction conditions. It is shown that the popular ADT protocol proposed by the FCCJ to simulate load-cycle conditions leads to suitable results for describing the degradation behavior of the catalyst, whereas the protocol proposed for simulating start-up/shutdown conditions leads to massive corrosion of the carbon in the catalyst layer, as well as the MPL and GDL, thereby obstructing the ability to track the surface area loss of the catalyst. Therefore, we propose a combination of the two protocols, limiting the number of high potential excursions as a feasible alternative. Such treatment would also be closer to a realistic condition, where not exclusively load-cycle or start-up/shutdown conditions are applied, but both cases occur. Using these ADT protocols a significant influence of the particle size on the ECSA loss is observed; although it is acknowledged that the (assumed) heat treatment of the catalyst also changes the carbon support. Furthermore, it is shown that the gas atmosphere (reactant or inert gas, as well as dry or humidified gas) influences the degradation behavior. In contrast to previous reports, it is demonstrated that the influence of the presence of oxygen on the degradation depends on the ADT protocol and the catalyst. No systematic difference between the liquid and polymer environment was seen; however, it is found that when applying high potential excursions, the influence of the reactant gas atmosphere becomes less pronounced (for those cases where a clear influence is observed).

More intriguing is the observed influence of the reactant humidity, which cannot be studied in conventional cells using liquid electrolytes. It is found that under dry conditions only parts of the catalyst layer participate in the reaction. In a potentiostatic ADT protocol, almost all of the initial surface area can be re-established by switching back to humidified conditions, i.e. the apparent loss in ECSA is reversible. This is, however, not the case in a more realistic amperometric degradation protocol. This finding highlights the fact that to investigate such effects, additional ADT protocols are needed to ensure that the entire catalyst layer is indeed participating in the reaction.

Last, but not least, it is demonstrated that the IL-TEM technique can easily be integrated in the measurements, allowing a combination of surface area loss determination and mechanistic insights. This is even possible at 60 °C, i.e. close to the actual operation temperature of a PEMFC. To sum up, it is demonstrated that the introduced GDE setup offers substantial advantages over standard degradation measurements in electrochemical cells employing liquid electrolytes.

Acknowledgments

This work was supported by the Swiss National Science Foundation (SNSF) via the project No. 200021_184742. M I and M A gratefully acknowledge support from Toyota Central R&D Labs., Inc. J S gratefully acknowledges the DFG for financial support (KU 3152/6-1).

ORCID iDs

Matthias Arenz  <https://orcid.org/0000-0001-9765-4315>

References

- [1] Gasteiger H A *et al* 2005 Activity benchmarks and requirements for Pt, Pt-alloy, and non-Pt oxygen reduction catalysts for PEMFCs *Appl. Catalysis B-Environ.* **56** 9–35
- [2] Borup R *et al* 2007 Scientific aspects of polymer electrolyte fuel cell durability and degradation *Chem. Rev.* **107** 3904–51
- [3] Mayrhofer K J J *et al* 2008 Fuel cell catalyst degradation on the nanoscale *Electrochem. Commun.* **10** 1144–7
- [4] Hartl K, Hanzlik M and Arenz M 2011 IL-TEM investigations on the degradation mechanism of Pt/C electrocatalysts with different carbon supports *Energy & Environ. Sci.* **4** 234–8
- [5] Mayrhofer K J J *et al* 2008 Non-destructive transmission electron microscopy study of catalyst degradation under electrochemical treatment *J. Power Sources* **185** 734–9
- [6] Lafforgue C *et al* 2019 Degradation of carbon-supported platinum-group-metal electrocatalysts in alkaline media studied by *in situ* Fourier transform infrared spectroscopy and identical-location transmission electron microscopy *ACS Catalysis* **9** 5613–22
- [7] Hodnik N and Cherevko S 2019 Spot the difference at the nanoscale: identical location electron microscopy in electrocatalysis *Curr. Opin. Electrochem.* **15** 73–82

- [8] Aran-Ais R M *et al* 2015 Identical location transmission electron microscopy imaging of site-selective Pt nanocatalysts: electrochemical activation and surface disordering *JACS* **137** 14992–8
- [9] Rasouli S *et al* 2019 Electrochemical degradation of Pt-Ni nanocatalysts: an identical location aberration-corrected scanning transmission electron microscopy study *Nano Lett.* **19** 46–53
- [10] Souza N E *et al* 2018 Support modification in Pt/C electrocatalysts for durability increase: a degradation study assisted by identical location transmission electron microscopy *Electrochim. Acta* **265** 523–31
- [11] Lafforgue C *et al* 2018 Accelerated stress test of Pt/C nanoparticles in an interface with an anion-exchange membrane—an identical-location transmission electron microscopy study *ACS Catalysis* **8** 1278–86
- [12] Kinumoto T *et al* 2015 Degradation of the Pt/C electrode catalyst monitored by identical location scanning electron microscopy during potential pulse durability tests in HClO₄ solution *Electrochemistry* **83** 12–7
- [13] Schuppert A K *et al* 2012 A scanning flow cell system for fully automated screening of electrocatalyst materials *J. Electrochem. Soc.* **159** F670–5
- [14] Kasian O *et al* 2018 Electrochemical on-line ICP-MS in electrocatalysis research *The Chemical Record* **19** 2130–42
- [15] Pizzutilo E *et al* 2016 On the need of improved accelerated degradation protocols (ADPs): examination of platinum dissolution and carbon corrosion in half-cell tests *J. Electrochem. Soc.* **163** F1510–4
- [16] Marcu A *et al* 2012 *Ex situ* testing method to characterize cathode catalysts degradation under simulated start-up/shut-down conditions—a contribution to polymer electrolyte membrane fuel cell benchmarking *J. Power Sources* **215** 266–73
- [17] Borup R L *et al* 2006 PEM fuel cell electrocatalyst durability measurements *J. Power Sources* **163** 76–81
- [18] Ohma A *et al* 2011 Membrane and catalyst performance targets for automotive fuel cells by FCCJ membrane, catalyst, MEA WG *ECS Trans.* **41** 775–84
- [19] Park Y-C *et al* 2013 Investigation of the corrosion of carbon supports in polymer electrolyte fuel cells using simulated start-up/shutdown cycling *Electrochim. Acta* **91** 195–207
- [20] Zana A *et al* 2013 Probing degradation by IL-TEM: the influence of stress test conditions on the degradation mechanism *J. Electrochem. Soc.* **160** F608–15
- [21] Ferreira P J *et al* 2005 Instability of Pt/C electrocatalysts in proton exchange membrane fuel cells—a mechanistic investigation *J. Electrochem. Soc.* **152** A2256–71
- [22] Kucernak A R and Toyoda E 2008 Studying the oxygen reduction and hydrogen oxidation reactions under realistic fuel cell conditions *Electrochem. Commun.* **10** 1728–31
- [23] Fleige M *et al* 2016 Evaluation of temperature and electrolyte concentration dependent Oxygen solubility and diffusivity in phosphoric acid *Electrochim. Acta* **209** 399–406
- [24] Fleige M J, Wiberg G K H and Arenz M 2015 Rotating disk electrode system for elevated pressures and temperatures *Rev. Sci. Instrum.* **86** 064101
- [25] Wiberg G K H, Fleige M J and Arenz M 2014 Design and test of a flexible electrochemical setup for measurements in aqueous electrolyte solutions at elevated temperature and pressure *Rev. Sci. Instrum.* **85** 085105
- [26] Pinaud B A *et al* 2017 Key considerations for high current fuel cell catalyst testing in an electrochemical half-cell *J. Electrochem. Soc.* **164** F321–7
- [27] Zalitis C M, Kramer D and Kucernak A R 2013 Electrocatalytic performance of fuel cell reactions at low catalyst loading and high mass transport *Phys. Chem. Chem. Phys.* **15** 4329–40
- [28] Nikkuni F R *et al* 2014 The role of water in the degradation of Pt₃Co/C nanoparticles: an identical location transmission electron microscopy study in polymer electrolyte environment *Appl. Catalysis B-Environ.* **156** 301–6
- [29] Zalitis C M *et al* 2015 Properties of the hydrogen oxidation reaction on Pt/C catalysts at optimised high mass transport conditions and its relevance to the anode reaction in PEFCs and cathode reactions in electrolyzers *Electrochim. Acta* **176** 763–76
- [30] Wiberg G K H, Fleige M and Arenz M 2015 Gas diffusion electrode setup for catalyst testing in concentrated phosphoric acid at elevated temperatures *Rev. Sci. Instrum.* **86** 024102
- [31] Inaba M *et al* 2018 Benchmarking high surface area electrocatalysts in a gas diffusion electrode: measurement of oxygen reduction activities under realistic conditions *Energy Environ. Sci.* **11** 988–94
- [32] Sievers G W *et al* 2019 Sputtered platinum thin-films for oxygen reduction in gas diffusion electrodes: a model system for studies under realistic reaction conditions *Surfaces* **2** 336–48
- [33] Higgins D *et al* 2019 Gas-diffusion electrodes for carbon dioxide reduction: a new paradigm *ACS Energy Letters* **4** 317–24
- [34] Wiberg G K H, Mayrhofer K J J and Arenz M 2010 Investigation of the oxygen reduction activity on silver—a rotating disc electrode study *Fuel Cells* **10** 575–81
- [35] Reiser C A *et al* 2005 A reverse-current decay mechanism for fuel cells *Electrochem. Solid State Lett.* **8** A273–6
- [36] Kangasniemi K H, Condit D A and Jarvi T D 2004 Characterization of vulcan electrochemically oxidized under simulated PEM fuel cell conditions *J. Electrochem. Soc.* **151** E125–32
- [37] Speder J *et al* 2013 On the influence of the Pt to carbon ratio on the degradation of high surface area carbon supported PEM fuel cell electrocatalysts *Electrochem. Commun.* **34** 153–6
- [38] Topalov A A *et al* 2014 The impact of dissolved reactive gases on platinum dissolution in acidic media *Electrochem. Commun.* **40** 49–53
- [39] Cheah S K *et al* 2011 CO impact on the stability properties of Pt_xCo_y nanoparticles in PEM fuel cell anodes: mechanistic insights *J. Electrochem. Soc.* **158** B1358–67
- [40] Franco A A *et al* 2009 Impact of carbon monoxide on PEFC catalyst carbon support degradation under current-cycled operating conditions *Electrochim. Acta* **54** 5267–79
- [41] Zana A *et al* 2013 Investigating the corrosion of high surface area carbons during start/stop fuel cell conditions: a Raman study *Electrochim. Acta* **114** 455–61
- [42] Schlogl K, Hanzlik M and Arenz M 2012 Comparative IL-TEM study concerning the degradation of carbon supported Pt-based electrocatalysts *J. Electrochem. Soc.* **159** B677–82
- [43] Makharia R *et al* 2006 Durable PEM fuel cell electrode materials: requirements and benchmarking methodologies *ECS Trans.* **1** 3–18
- [44] Speder J *et al* 2013 Pt based PEMFC catalysts prepared from colloidal particle suspensions—a toolbox for model studies *Phys. Chem. Chem. Phys.* **15** 3602–8
- [45] Castanheira L *et al* 2015 Carbon corrosion in proton-exchange membrane fuel cells: effect of the carbon structure, the degradation protocol, and the gas atmosphere *ACS Catalysis* **5** 2184–94